

Aberrant fast spiking interneuronal activity precedes seizure transitions in humans:

Supplementary Information

Edward M. Merricks^{1✉}, Sarita S. Deshpande^{2,3,4}, Alexander H. Agopyan-Miu⁵, Elliot H. Smith^{1,6}, Emily D. Schlafly⁷, Guy M. McKhann II⁵, Robert R. Goodman⁸, Sameer A. Sheth⁹, Bradley Greger¹⁰, Paul A. House¹¹, Emad N. Eskandar¹², Joseph R. Madsen^{13,14}, Sydney S. Cash¹⁵, Andrew J. Trevelyan¹⁶, Wim van Drongelen^{3,4,17}, Catherine A. Schevon^{1✉}

¹ Department of Neurology, Columbia University Medical Center, New York, NY 10032

² Medical Scientist Training Program, University of Chicago, Chicago, IL 60637

³ Committee on Neurobiology, University of Chicago, Chicago, IL 60637

⁴ Section of Pediatric Neurology, University of Chicago, Chicago, IL 60637

⁵ Department of Neurological Surgery, Columbia University Medical Center, New York, NY 10032

⁶ Department of Neurosurgery, University of Utah, Salt Lake City, UT 84132

⁷ Graduate Program in Neuroscience, Boston University, Boston, MA 02215

⁸ Department of Neurosurgery, Hackensack Meridian School of Medicine, Nutley, NJ 07110

⁹ Department of Neurosurgery, Baylor College of Medicine, Houston, TX 77030

¹⁰ School of Biology and Health Systems Engineering, Arizona State University, Tempe, AZ 85287

¹¹ Intermountain Healthcare, Murray, UT 84107

¹² Department of Neurological Surgery, Montefiore Medical Center, Bronx, NY 10461

¹³ Department of Neurosurgery, Massachusetts General Hospital & Harvard Medical School, Boston, MA 02114

¹⁴ Department of Neurosurgery, Brigham and Women's Hospital & Harvard Medical School, Boston, MA 02115

¹⁵ Department of Neurology, Massachusetts General Hospital & Harvard Medical School, Boston, MA 02114

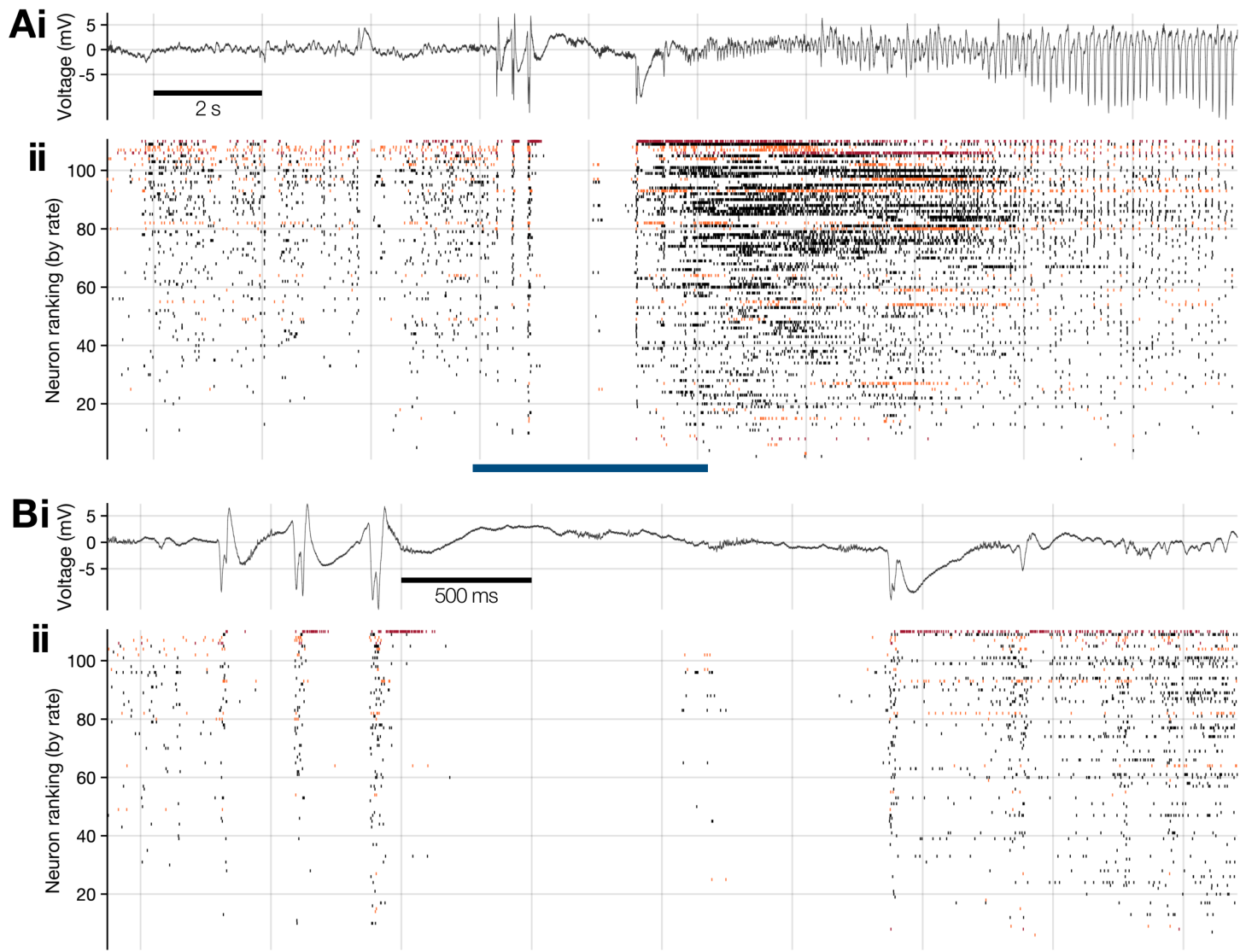
¹⁶ Newcastle University Biosciences Institute, Newcastle upon Tyne, United Kingdom, NE2 4HH

¹⁷ Committee on Computational Neuroscience, University of Chicago, Chicago, IL 60637

✉ e-mail: em3217@cumc.columbia.edu (EMM); cas2044@cumc.columbia.edu (CAS)

Contents

- Supplementary Figure 1
- Table S1
- Table S2
- Table S3
- Supplementary Movie 1 legend
- Supplementary Movie 2 legend



Supplementary Figure 1. Neuronal firing underlying a spontaneous, human focal seizure. **(a)(i)** Mean LFP calculated across the Utah array during patient 4's seizure, bandpass filtered between 2–50 Hz. **(ii)** Underlying, time-locked neuronal firing across the full Utah array, tracked with convex hulls²⁸, ordered by each neuron's firing rate during the epoch, with putative pyramidal cells in black, "wide" interneurons in orange, and FS interneurons in red. **(b)** Enlargement of the epoch marked with a blue bar in (a), using the same layout.

Patient	Age range	Sex	MEA length (mm)	Implant location	Seizure onset	Pathology	Seizure #	Seizure type	Rhythmic onset	Evidence of recruitment	Total neurons	Total FS interneurons
1	26–30	M	1.0	Left frontal convexity	Left supplementary motor area	Nonspecific	1	FIA	-	N	75	0
							2	FIA	-	N	75	0
							3	FIA	-	N	50 (-4)	1
2	36–40	M	1.0	Left dorsolateral frontal lobe	Left frontal operculum	Nonspecific	1	FIA	-	N	61	3
							2	FIA	-	N	65	2
							3	FIA	-	N	59 (-2)	0
3	31–35	F	1.0	Left inferior temporal gyrus	Left basal/anterior temporal	Mild CA1 neuronal loss; lateral temporal nonspecific	1	FIA	Y	Y	111	17
							2	FIA	Y	Y	101	3
							3	FIA	Y	Y	91	6
4	18–25	F	1.0	Right posterior temporal gyrus	Right posterior lateral temporal	Nonspecific	1	FTBTC	-	Y	110	1
5	26–30	M	1.0	Left premotor	Left prefrontal	Mild reactive astrogliosis; patchy microgliosis; Chaslin's marginal sclerosis	1	FTBTC	Y	Y	120	9
							2	FTBTC	-	Y	309	15
6	26–30	M	1.0	Left posterior inferior temporal gyrus	Left subtemporal/lateral temporal	Diffusely infiltrating low grade glioma, IDH-1 negative	1	FIA	Y	Y	165	9
							2	FIA	Y	Y	104	10
							3	FIA	-	Y	102	11
7	26–30	M	1.0	Right mesial temporal gyrus	Right subtemporal	Mild astrocytosis	1	FA	-	Y (partial)	240	19
							2	FA	-	Y	252 (-16)	13 (-2)
							3	FA	-	Y	241	14
8	26–30	M	1.0	Left anterior/inferior temporal	Left frontal polar/orbitofrontal	Focal cortical dysplasia type 2a; Reactive astrogliosis	1	FIA	-	Y	77	7
							2	FTBTC	-	Y	78	11
							3	FTBTC	-	Y	77	1
9	18–25	M	1.0	Left inferior temporal gyrus	Left mesial temporal with spread to lateral temporal	Mesial temporal sclerosis; nonspecific	1	FIA	Y	Y	119 (-1)	9
							2	FIA	Y	Y	133	14
10	31–35	M	1.0	Right inferior frontal gyrus	Right mesial temporal	Nonspecific	1	FTBTC	Y	Y	86	4
11	41–45	M	1.5	Right middle temporal gyrus	Right temporal	Mesial temporal sclerosis	1	FTBTC	Y	Y	109	10
							2	FTBTC	Y	Y	83	5
							3	FTBTC	Y	Y	137	7
12	31–35	M	1.5	Left middle temporal gyrus	Mesial temporal	Mesial temporal sclerosis	1	FIA	Y	Y	234	11
							2	FIA	Y	Y	189	10
							3	FIA	Y	Y	230	14
13	18–25	M	1.0	Left superior temporal gyrus	Left temporal	Mesial temporal sclerosis	1	FIA	Y	Y	121	10
							2	FIA	Y	Y	91	5
							3	FIA	Y	Y	104	5

Table S1. Patient demographics. Numbers in parentheses represent total neurons that were not trackable during the seizure via convex hull template matching²⁸. FTBTC = focal to bilateral tonic clonic; FIA = focal with impaired awareness; FA = focal aware.

Cellular parameters

	Resonator	Integrator	Units
Capacitance	1	3	$\mu\text{F}/\text{cm}^2$
E_{Na}	55	50	mV
E_{K}	-72	-95	mV
E_{L}	-49.4	-63.7	mV
g_{Na}	120	25	mS/cm^2
g_{K}	36	5	mS/cm^2
g_{L}	0.3	0.1	mS/cm^2

Table S2. Cellular parameters used in Hodgkin-Huxley model. Values reproduced/scaled from Bukoski *et al.*⁶⁰

Symbol	Resonator	Integrator
$\alpha_n(V)$	$0.01(V + 50)/\{1 - \exp[-(V + 50)/10]\}$	$-0.032(V + 50)/\{\exp[-(V + 50)/5] - 1\}$
$\alpha_m(V)$	$0.1(V + 35)/\{1 - \exp[-(V + 35)/10]\}$	$-0.0053(V + 52)/\{\exp[-(V + 52)/4] - 1\}$
$\alpha_h(V)$	$0.07 \exp[-(V + 60)/20]$	$0.128 \exp[-(V + 48)/18]$
$\beta_n(V)$	$0.125 \exp[-(V + 60)/80]$	$0.084 \exp[-(V + 55)/40]$
$\beta_m(V)$	$4 \exp[-(V + 60)/18]$	$0.28(V + 25)/\{\exp[(V + 25)/5] - 1\}$
$\beta_h(V)$	$1/\{\exp[-(V + 30)/10] + 1\}$	$4/\{\exp[-(V + 25)/5] + 1\}$

Table S3. Gating equations for resonator and integrator classes. Reproduced/scaled from Bukoski *et al.*⁶⁰

Supplementary Movie Legends:

Supplementary Movie 1. Fast-spiking interneuron activity during ictal propagation, with successful inhibitory restraint. Above: Mean LFP from the Utah array during patient 7's first seizure, with "global" onset and current time marked (blue triangle and red line respectively). Below: A heatmap showing the 2-dimensional linear regression fit to all excitatory cells' spike full-width at half-maximum (FWHM; z-axis and heatmap color) with respect to their location on the Utah array (x- and y-axes), at each moment in time (5 s window, advancing in 100 ms steps). Each red dot embedded in the plane represents one fast-spiking (FS) interneuron, with the diameter showing that cell's instantaneous firing rate. Note the increase in inhibitory activity across the array shortly after global seizure onset (~15 seconds through movie), the approaching ictal wavefront at the nearest corner ($x = 3.6$ mm, $y = 0.0$ mm; ~27 seconds; represented by an increase in the excitatory population FWHM), followed by sudden reductions in nearby FS interneuron firing rates ahead of the ictal wavefront propagating into that region (~30 seconds till end). Note only half the array was successfully recruited to the seizure before termination, with maintained FS inhibitory firing outside the recruited region (c.f. Fig. 2 in main text).

Supplementary Movie 2. Fast-spiking interneuron activity during ictal propagation across whole array. Same design and layout as Supplementary Movie 1, using patient 7's second seizure, where the seizure managed to spread across the full Utah array prior to ictal termination. Note the increasing FS interneuron firing rates just prior to the excitatory population's FWHM increase, and their collapse as the local excitatory population FWHM reaches its peak at each location, with a temporal progression from right to left.